REVIEW

National Science Review
5: 144–158, 2018
doi: 10.1093/nsr/nwy017
Advance access publication 23 January 2018

PHYSICS

Special Topic: Metamaterials

All-dielectric meta-optics and non-linear nanophotonics

Yuri Kivshar[1,2]

ABSTRACT

Most optical metamaterials fabricated and studied to date employ metallic components resulting in significant losses, heat and overall low efficiencies. A new era of metamaterial physics is associated with *all-dielectric meta-optics*, which employs electric and magnetic Mie resonances of subwavelength particles with high refractive index for an optically induced magnetic response, thus underpinning a new approach to design and fabricate functional and practical metadevices. Here we review the recent developments in meta-optics and subwavelength dielectric photonics and demonstrate that the Mie resonances can play a crucial role in the realization of the unique functionalities of meta-atoms, also driving novel effects in the fields of metamaterials and nanophotonics. We discuss the recent research frontiers in all-dielectric meta-optics and uncover how Mie resonances can be employed for a flexible control of light with full phase and amplitude engineering, including unidirectional metadevices, highly transparent metasurfaces, non-linear nanophotonics and topological photonics.

Keywords: nanophotonics, Mie resonances, meta-optics, metasurfaces, metamaterials

INTRODUCTION

Electromagnetic metamaterials, artificial media in which subwavelength electromagnetic constituents replace atoms as the basic structural elements to control the light–matter interaction, have led to the prediction and observation of many novel optical phenomena that are not available or are much weaker in natural materials [1–5]. This includes a negative index of refraction, invisibility cloaking, giant chirality, etc. Many such important phenomena are the manifestation of *optical magnetism*, predicted and observed in specifically designed artificial subwavelength structures that allow a strong magnetic response, even when such structures are made of non-magnetic materials. Indeed, although real quantum-origin magnetism in its conventional sense is not available at high optical frequencies, the metamaterial concept allows the design of artificial 'meta-atoms' to engineer macroscopic magnetic permeability μ and magnetic response by achieving strong resonances in structured non-magnetic systems, through the spatial dispersion and non-local electric-field effects, inducing a strong magnetic-dipole moment.

The most popular constitutive elements of metamaterials are split-ring resonators, cut-wire pairs and metal–dielectric layered structures with the so-called fishnet geometry [3]. Such classical 'meta-atoms' are made of metals where free electrons oscillate back and forth, creating effective loops of current, thus inducing an efficient magnetic response. The meta-atom in the form of a split-ring resonator was first introduced at microwaves to realize artificial magnetically active inclusions with subwavelength footprints, and then it was translated to the optics exploiting the plasmonic features of metallic nanoparticles [3]. This concept was realized in many non-magnetic plasmonic structures ranging from nanobars [6] and nanoparticle oligomers [7,8] to split-ring-based structures [9,10] and more complex metal–dielectric layered structures associated with hyperbolic-type electric and magnetic response of metamaterials [11,12]. These earlier results created a platform for the subsequent development of the entirely new fields of metadevices [13] as well as metasurfaces and metalenses [14,15].

The idea of using metallic elements in metamaterials is based on the main assumption that the

[1]Nonlinear Physics Center, Australian National University, Canberra ACT 2601, Australia and [2]ITMO University, St Petersburg 197101, Russia

E-mail: ysk@physics.anu.edu.au

Received 3 October 2017; **Revised** 15 January 2018; **Accepted** 16 January 2018

subwavelength trapping of light may occur due to the localization of electromagnetic waves at metallic interfaces in the form of *surface plasmon polaritons*. Plasmonic resonators are always accompanied by losses because of their response nature: in order to achieve the resonant behavior for subwavelength plasmonic resonators, part of the optical energy must be stored in the kinetic energy of electrons [16]. Even high-T_c superconductors cannot be a good alternative for noble metals because they would have to operate at energies less than the superconductive gap, being in the THz or far-IR frequency range [17]. The use of highly doped semiconductors in place of metal is also not a panacea because the decline of the Fermi level necessarily means a decrease in the plasma frequency and, thus, lowering of surface and localized plasmonic resonances, where the noble metals demonstrate superior properties. In particular, doped semiconductors with lower losses have been proposed as new plasmonic materials to replace noble metals [18–20]. However, recent studies suggest that noble metals outperform doped semiconductors even with their larger ohmic losses because of the inherently higher plasma frequencies in metals. While the intrinsic loss in doped semiconductors can be an order of magnitude lower than in metals, their electron densities and thus plasma frequencies are at least thirty times smaller.

By now, it has become clear that practically useful methods to control light–matter interactions at the nanoscale need to go beyond plasmonics. Probably the most disruptive strategy would be to replace metals by *all-dielectric components* with high refractive index, supporting the light localization due to dielectric resonators, and provide fine control over the amplitude, phase and polarization of light. Because this approach requires nanostructures of the order of a few hundred nanometers, the ability to describe composite media by averaged parameters via the homogenization procedure can be lost, so such structures should be classified from the viewpoint of *'meta-optics'* rather than *'metamaterials'*. On the other hand, the use of silicon and other semiconductors brings the great advantage of CMOS compatibility that will be appreciated in practical applications [21].

The recent developments of the physics of high-index dielectric nanoparticles [22–25] suggest the importance of an alternative mechanism of light localization in subwavelength optical structures via low-order dipole and multipole Mie resonances [26] that may generate magnetic response via the displacement current contribution. The study of resonant dielectric nanostructures has been established as a new research direction in modern nanoscale optics and metamaterial-inspired nanophotonics [22–24]. Because of their unique optically induced electric and magnetic geometry-driven resonances, high-index nanophotonic structures are expected to complement or even replace different plasmonic components in a range of potential applications.

The aim of this invited review paper is twofold. First, we provide a broad view of the rapidly developing field of *all-dielectric resonant meta-optics*, uncovering a great potential of optically induced electric and magnetic Mie resonances for the design of novel types of low-loss optical metasurfaces and metadevices. Second, we discuss briefly two emerging fields of *multipolar non-linear nanophotonics* and *topological optics* based on the engineering of high-index subwavelength dielectric nanoparticles, their arrays, lattices and meta-crystals, which employ both electric and magnetic resonant modes. We envisage the rapid progress of all these fields for achieving flexible control of light with all-dielectric metamaterials, metasurfaces and metadevices.

METAMATERIALS AND MIE RESONANCES

Magnetic response

As mentioned above, the magnetic response of many natural materials at optical frequencies is very weak. Thus, only the electric component of light is directly controlled in many optical devices. However, artificial magnetism can be achieved at high frequencies in nanostructured materials. One of the canonical examples is the split-ring resonator (SRR), shown in Fig. 1(a), an inductive metallic ring with a gap (a building block of a majority of metamaterials) that can support an oscillating current, giving rise to an optically induced magnetic moment. However, intrinsic losses of metals set the fundamental limit for the use of SRRs at optical frequencies. This is where high-index dielectric (e.g. silicon) nanoparticles of hundreds of nanometers make an attractive alternative [27]. According to the Mie theory, dielectric nanoparticles can exhibit strong magnetic resonances in the visible [28]. The basic physics of the excitation of such modes is similar to that of SRRs, provided that the electron current in metals is replaced by the displacement current in dielectrics, but silicon nanoparticles have much lower losses. A magnetic resonance originates from the excitation of a particular electromagnetic mode inside the nanoparticle with a circular displacement current of the electric field. This mode is excited when the wavelength of light in the material becomes comparable to the particle's diameter. It has an antiparallel polarization of the electric field at opposite sides of the particle while the magnetic field oscillates up and down in the middle [29] (see Fig. 1(b)).

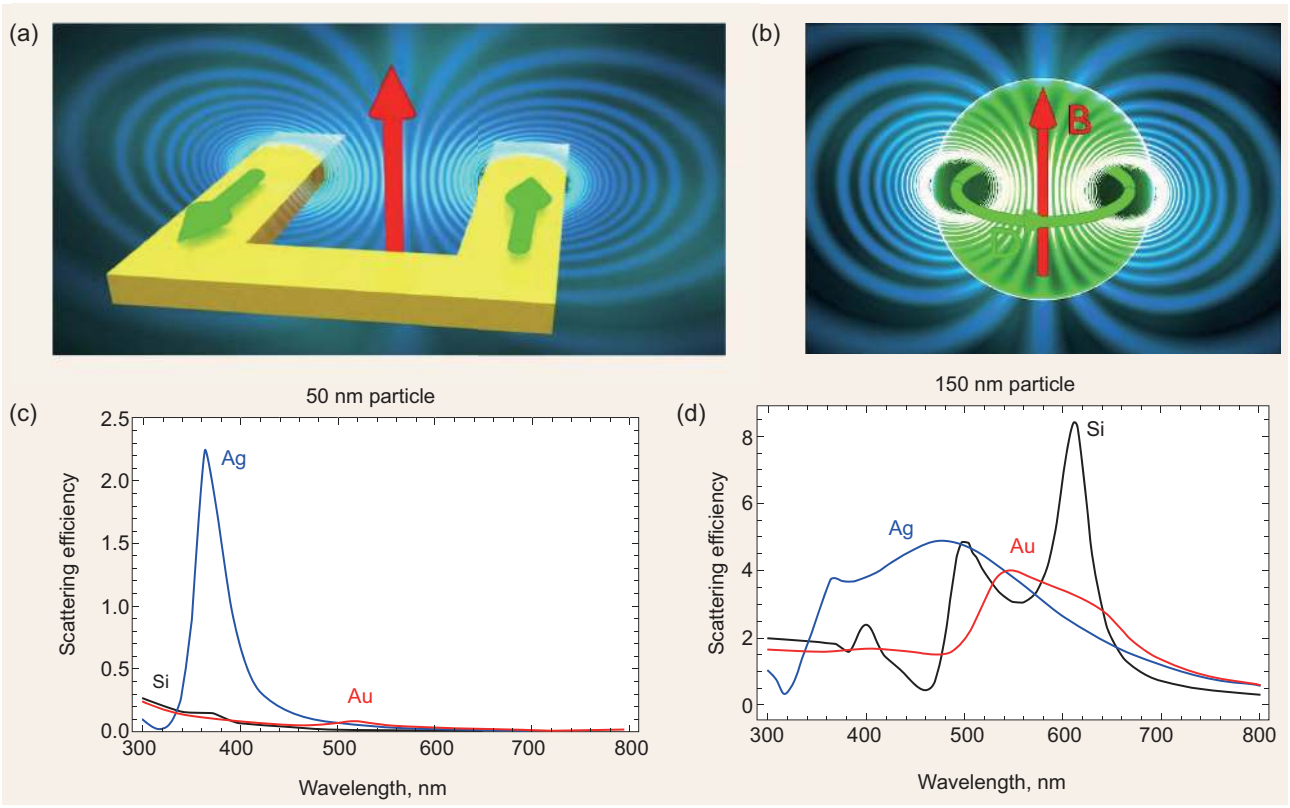

Figure 1. Optically induced magnetic response. (a), (b) Schematic of magnetic-dipole moments excited in a metallic split-ring resonator and high-index dielectric nanoparticle. (c), (d) Comparison of the scattering cross sections of gold (Au), silver (Ag) and silicon (Si) nanoparticles of the same geometrical shapes and diameters of (c) 50 nm and (d) 150 nm, respectively. These results suggest that, in addition to a new type of resonances, dielectric particles scatter light more efficiently than plasmonic nanoparticles of larger sizes [27].

This fundamental phenomenon of strong magnetic resonances in optics was independently observed experimentally throughout the whole visible spectral range from violet to red for silicon nanoparticles with sizes ranging from 100 to 270 nm [30] and 200 to 265 nm [31]. Thus, it makes silicon nanoparticles good candidates for lossless magnetic response at high frequencies and lossless metamaterials, in sharp contrast to plasmonic nanoparticles of the same size and geometry [27] (see Fig. 1(c) and (d)).

Dielectric nanoparticles with strong magnetic response can be used as building blocks to explore new types of multipolar interaction at the nanoscale [32]. Coupling of silicon nanoparticles and SRRs allows control of the magnetic interaction between optically induced dipole moments. If the spacing between a nanoparticle and an SRR becomes smaller than a critical value, the induced magnetization can be inverted [33,34]. This approach can be generalized to construct a variety of hybrid structures supporting and controlling optically induced spin waves.

In the visible and near-IR spectral ranges, large permittivity is known to occur for semiconductors such as Si, Ge and AlGaAs. In the neighboring mid-IR range, which is also of great interest to nanophotonics, narrow-band semiconductors (Te and PbTe) and polar crystals such as SiC can be implemented for all-dielectric resonant metadevices driven by Mie resonances. A search for better materials and fabrication techniques for high-index dielectric nanophotonics is an active area of research [21].

Multipolar interference effects

To understand the major characteristics of light scattering at the nanoscale, one usually employs the multipole decomposition of electromagnetic fields. In this way, the Mie scattering is characterized by partial intensities and radiation patterns of dominant excited multipole modes, not only the electric and magnetic dipoles but also higher-order multipolar modes and modes with toroidal geometry. For metallic nanoparticles, the electric-dipole mode usually dominates the Mie scattering. In contrast, incorporating the optical magnetic response for dielectric particles provides an extra degree of freedom for efficient light control, through interference of electric and magnetic dipoles and multipolar modes.

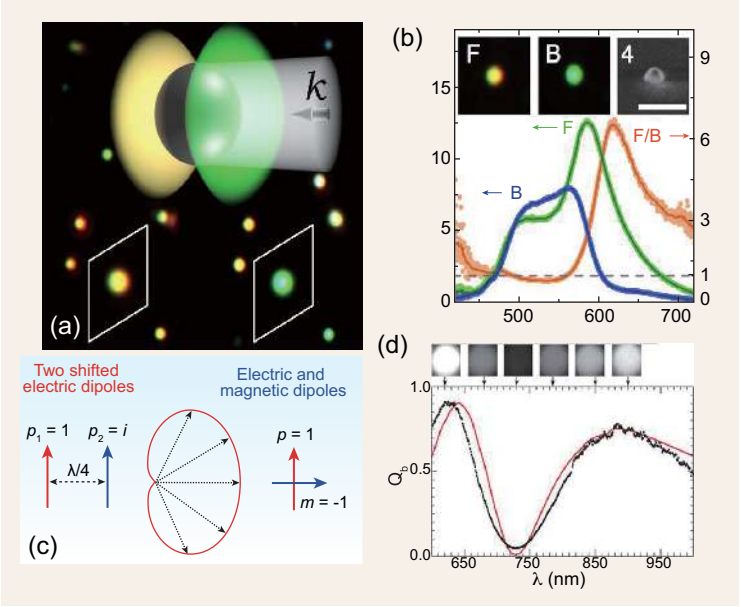

Figure 2. Unidirectional scattering of light. (a) CCD images of the forward and backward scattering by Si nanoparticles and (b) the experimentally measured forward-to-backward ratio [43]. (c) Schematic of two physical mechanisms leading to unidirectional scattering. (d) Experimentally measured (black) and numerically calculated (red) backscattering spectrum from a single GaAs nanodisk [44].

In the simplest case, when multipole modes are of the same type and are produced by different elements, the interference physics of dielectric nanoparticles is associated with *Fano resonances*, and it resembles plasmonic analogues [35]. Nanoparticle structures demonstrate sharp Fano resonances with characteristic asymmetric scattering due to interference between non-radiative and radiative modes. Importantly, magnetic-dipole resonances of individual dielectric particles play a crucial role in the appearance of the Fano resonances [36–38].

The possibility of exciting simultaneously both magnetic- and electric-dipole modes may lead to entirely *new classes of scattering phenomena*. Kerker [39] revealed that it is possible to suppress the backscattering by using a hypothetical nanoparticle made of a material with identical electric permittivity ϵ and magnetic permeability μ. This condition implies that two excited dipole modes have equal amplitudes, and they interfere destructively in the backward direction.

This type of interference between two optically induced dipole-mode resonances and Kerker's condition can be realized in layered core–shell nanoparticles with metal cores and dielectric shells [40]. A superposition of electric and magnetic resonances of a single core–shell nanoparticle results in the suppression of the backward scattering and unidirectional emission by a single subwavelength element [40]. The directivity of emission can be further enhanced by forming a chain of such nanoparticles.

Importantly, the unique property of the unidirectional scattering and Kerker conditions (see Fig. 2(a) and (b)) can be found in dielectric nanoparticles [41,42], which allow the introduction of a novel concept of optical nanoantennas made of high-permittivity dielectric nanoparticles. Such all-dielectric nanoantennas exhibit much higher radiation efficiency, allowing more practical design compared to their plasmonic counterparts.

Thus, nanoparticles made of low-loss high refractive index dielectric materials offer a promising solution for a new generation of metadevices, also removing many severe limitations of plasmonic structures but exhibiting a strong resonant response at the nanoscale. The key to such novel functionalities of high-index dielectric nanophotonic elements is the ability of subwavelength dielectric nanoparticles to support simultaneously both electric and magnetic resonances, which can be controlled independently [43,44].

To explain the basic physics of these novel interference effects, we remind ourselves that, in the Rayleigh approximation, any single subwavelength element radiates light as an electric dipole, i.e. uniformly in the transverse direction relative to the dipole orientation. Thus, to control any radiation pattern, one needs to have at least two elements and take advantage of the interference of their radiative fields. An ideal optical nanoantenna would emit light predominantly in one predefined direction. The simplest structure exhibiting a unidirectional radiation pattern consists of two dipoles separated by a quarter of a wavelength with an additional $\pi/2$ phase shift between them (see Fig. 2(c)). It turns out that waves generated by such a dipole pair interfere constructively in one direction and destructively in the opposite direction. However, the interference condition implies that the system's size should remain of the order of a wavelength.

Dielectric nanoparticles with high refractive index offer new possibilities for achieving wave interference. Indeed, the coexistence of both electric and magnetic resonances results in unidirectional scattering (see Fig. 2(a)). This property makes subwavelength dielectric nanoparticles the smallest and most efficient nanoantennas. Moreover, unidirectionality can be swapped for different wavelengths. In particular, Fu *et al.* [43] and Person *et al.* [44] measured the forward and backward radiation patterns of spherical Si nanoparticles with radii ranging from 50 nm to 100 nm exhibiting resonance behavior; see Fig. 2(b) and (d).

Metasurfaces

Huygens' principle, formulated in the 17th century, assumes that every point on a wavefront becomes

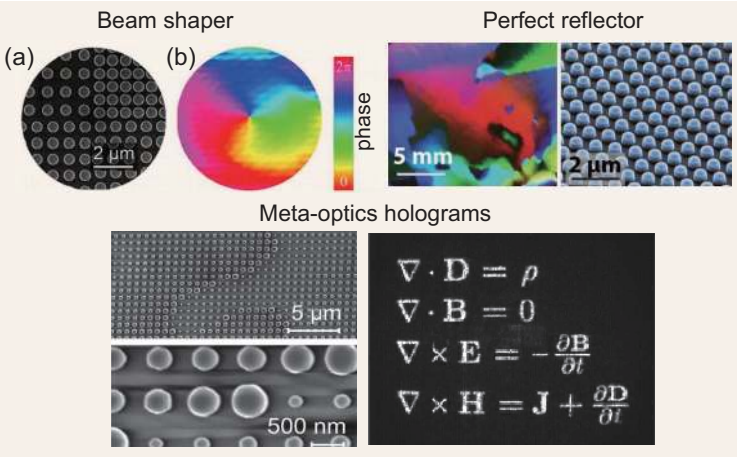

Figure 3. Examples of dielectric metasurfaces. Top left: (a), (b) SEM image of a fabricated silicon Huygens' metasurface (that transforms a Gaussian beam into a vortex beam), with a retrieved phase of the generated vortex beam, respectively [48]. Top right: Optical microscope and SEM images of a metasurface-based perfect reflector [53]. Bottom: SEM images of the fabricated meta-optics holograms and an experimental holographic image at 1600 nm wavelength [57].

the source of a secondary, forward-propagating wave. Despite its simplicity, this well-known principle intuitively explains why shaping of a wavefront requires imprinting a spatially variant phase distribution onto an incident light field. Control over the wavefront of light is the key to many optical functionalities including focusing, beam shaping, beam deflection and holographic imaging. While conventional optical components providing these functionalities are rather bulky, optical metasurfaces (2D arrangements of designed nanophotonic building blocks) allow for wavefront shaping using just a sheet of nanoscale thickness. Metasurfaces consisting of planar arrangements of designed nanoresonators are of particular interest, as they can provide many degrees of freedom not supported by conventional phase masks, such as a tailored polarization response or engineered spatial or spectral dispersion. However, typically such metasurfaces exhibit a very low transmission at resonance because, unlike the fictitious secondary sources of Huygens' principle, the fields scattered by the nanoresonators are not forward-propagating.

In the last few years, a new way has been demonstrated to shape the wavefront of a light field with close-to-unity efficiency and full phase coverage. The very efficient approach to create highly transparent metasurfaces is based on disk-shaped silicon nanoresonators carefully designed to exhibit spectrally overlapping electric and magnetic dipolar Mie-type resonances [45]. Such nanoresonators scatter the incoming light almost entirely in the forward direction, thereby mimicking the forward-propagating behavior of the elementary Huygens' sources [41,46] and making the metasurface highly transparent at the resonance. Furthermore, by using silicon as a constituent material, absorption losses become negligible at near-infrared operation wavelengths, thus boosting the metasurface efficiency compared to intrinsically lossy plasmonic metasurfaces. In combination, all the typical major loss channels of transmitting metasurfaces are eliminated in these silicon Huygens' metasurfaces [47].

To demonstrate this concept for wavefront shaping with high efficiency, Chong *et al.* [48,49] designed, fabricated and characterized several wavefront-shaping metadevices (see also some related earlier [50] and more recent [51] papers). In order to implement the desired space-variant distribution of transmittance phases, they varied the lattice constant of the silicon nanoresonator arrays as a function of the in-plane sample position; see Fig. 3(a) and (b). This allows the transmission to be kept high enough, while covering a large phase range. Both devices have experimental transmittance efficiencies exceeding 70% and work for any input polarization. Furthermore, they demonstrated tuning of the resonance wavelength of silicon nanoresonator arrays using liquid crystals [52], paving the way towards dynamic wavefront control. Altogether, silicon Huygens' metasurfaces offer important opportunities for efficient, flat and lightweight photonic devices.

Dielectric metasurfaces based on silicon nanodisks have emerged as a versatile tool for various applications since they support strong electric and magnetic modes that can be tailored in every relevant aspect—like resonance position, quality factor and resonance strength—by tailoring their shape and their arrangement within the metasurface. Utilizing the strong dipolar response of the nanoparticles, it is possible to realize ultrathin perfect metasurface-based reflectors with a reflectance of 99.7%, even surpassing the reflectance of metallic mirrors, at 1530 nm wavelength with a bandwidth of 200 nm [53]; see Fig. 3.

Importantly, metadevice multiplexers made of all-dielectric metasurfaces can be employed for engineering the mode profiles of arbitrary complexity, including Eisenbud–Wigner–Smith states [54] and orbital angular momentum modes [55]. Highly transparent all-dielectric resonant metasurfaces can be employed for engineering the mode profiles with high efficiency, e.g. for the conversion of LP_{01} modes into LP_{11} and LP_{21} modes for free-space optical communication [56]. In this way, a single metasurface is capable of mode-multiplexing with an extinction ratio in excess of 20 dB over the C-band with negligible penalty even for 100 Gb/s signals. The metasurface is expected to introduce no

performance degradation except for an excess loss due to reflections that can be minimized by applying an antireflective coating.

Multipolar effects can also be employed successfully for achieving the broadband operation of meta-optics holograms [57]. Today, we are witnessing an exciting rise in holographic optics driven by the enormous progress in our ability to structure materials at the nanoscale. This enables a new way to create highly efficient holograms with single-step patterning. Attracting concepts of complex wavefront engineering and multimodal resonant response, Wang *et al.* [57] designed highly transparent silicon holograms that allow high-resolution images to be encoded; see Fig. 3 (bottom).

Finally, we mention one more important development in the physics and applications of all-dielectric resonant metasurfaces for creating color pixels for bright field full color print [58–61]. Printing technology based on plasmonic structures has many advantages over pigment-based color printing, such as high resolution and low power consumption. However, due to high losses of metals in the visible spectrum, it becomes challenging to produce well-defined colors. Planar structures of dielectric nanoresonators enable high-quality resonances in the visible spectral range, and they can be employed for high-quality colors with selective wavelengths. Structural colors can be conveniently produced by nanoscale structuring of high-index dielectric materials. Compared to plasmonic analogs, color surfaces with high-index dielectrics, such as Si and Ge, have a lower reflectance and superior color contrast [61]. Laser-printable high-index dielectric color metasurfaces are scalable to a large area and open a new paradigm for printing and decoration with non-fading and vibrant colors.

Metamaterials

The idea of employing Mie resonances for building 3D metamaterials with low losses is relatively old, and a number of papers have suggested employing dielectric resonators for achieving magnetic response in bulk structures [62,63], with experimental demonstrations at microwaves [64–66]. Scaling such structures to optical wavelengths requires materials with high refractive index, and quite often they become inconsistent with the major concepts of the metamaterial physics based on homogenization and averaged parameters.

Being made of a periodic lattice of dielectric elements, all-dielectric metamaterials resemble closely their relatives, photonic crystals. However, these two types of periodic structures are usually considered in different physics regimes: 'metamaterials' are often associated with averaged parameters and negative refractive index, so it is silently assumed that they operate either in the long-wavelength limit or far from the Bragg resonances, whereas 'photonic crystals' have been introduced to create bandgaps, and the properties of Bragg scattering are important. Because such regimes can be realized in one structure by varying its parameters, such as permittivity and lattice constant, the more general term 'meta-crystal' is sometimes employed.

Things become more complex when each of the dielectric elements supports Mie resonances in the bandgap frequency range. To illustrate the physics of the associated phenomena, we notice that Rybin *et al.* [67] discussed a transition between photonic crystals and dielectric metamaterials and introduced the concept of a phase diagram, based on the physics of Mie and Bragg resonances. They revealed that a periodic photonic structure transforms into a metamaterial when the Mie gap opens up below the lowest Bragg bandgap, where the homogenization approach can be justified and the effective permeability becomes negative. That theoretical prediction was confirmed by microwave experiments for a meta-crystal composed of tubes filled with heated water [67]. This analysis provides a useful tool for designing different classes of electromagnetic materials with variable parameters.

Unlike metasurfaces operating at the normal or weakly oblique propagation of incoming light, 3D resonant dielectric structures operate at different angles, and in a majority of cases they are not described by averaged parameters introduced via the homogenization procedure. As mentioned above, such structures should be classified from the viewpoint of 'meta-optics', where subwavelength elements support various resonances and may be employed for the control of the light propagation, in contrast to effective media described by averaged parameters.

NON-LINEAR META-OPTICS

Second-harmonic generation (SHG) is one of the most important non-linear processes in optics. In SHG, the frequency of an incident light beam is doubled inside of a non-linear crystal, as shown schematically in Fig. 4(a) and (b). SHG is nowadays employed in many applications, including laser sources and non-linear microscopy. The simplest example is a green laser pointer employing an efficient frequency-doubling non-linear crystal and emitting light at 532 nm.

Usually, non-linear optics relies on bulk non-linear crystals, such as lithium niobate. Unfortunately, these materials are difficult to integrate with other devices, due to the difficulties inherent in their manufacturing and machining, and they are also not

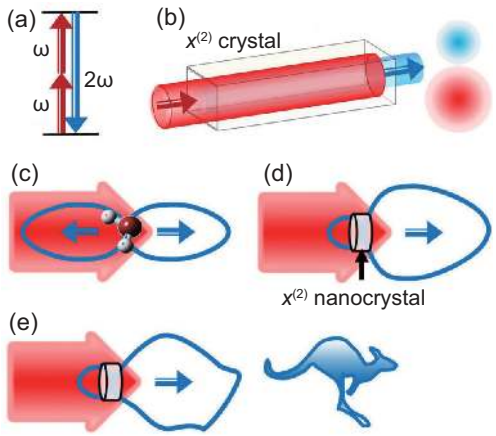

Figure 4. Non-linear optics: micro versus nano. (a) Schematic of SHG. (b) A conventional SHG process within a bulk non-linear crystal, generating a blue light in the forward direction. (c) SHG from small objects, such as anisotropic molecules, is emitted in both forward and backward directions, resulting in a dipolar radiation. (d) For larger nanocrystals, the emission can differ in forward and backward directions due to the interference of several multipoles inside the nanocrystal. (e) SHG from small nanocrystals with a designed radiation pattern and complex beam shape with high conversion efficiency (adapted from Ref. [68]).

cost-effective. Furthermore, special phase-matching conditions are often required in order to obtain useful conversion efficiencies. Although the output beam profile in bulk crystals can be engineered by complex periodic poling, this technique is not easily accessible due to its requirement for a spatially inhomogeneous distribution of high voltages across the crystals.

To overcome these issues, it would be useful if we could replace bulk non-linear crystals with ultrathin surfaces composed of nanocrystals that can generate SHG with high efficiency. Such non-linear meta-atoms could also be used to manipulate the SHG radiation to form complex beams with arbitrary patterns, as shown schematically in Fig. 4(c)–(e).

Recent progress of meta-optics suggest that AlGaAs nanocrystals fabricated on a glass substrate not only enable a non-linear conversion efficiency exceeding 10^{-4} (for subwavelength-thick structures), but also provide an opportunity to define the beam shape and polarization in both forward and backward directions [68]. The generation of complex and high-efficiency vector beams offers unique opportunities for many novel applications such as non-linear microscopy, non-linear holography, sum-frequency and difference-frequency generation, spontaneous parametric down-conversion, and parametric amplification. A wide range of opportunities requires much deeper studies of non-linear optics at the nanoscale.

General formalism

Within the macroscopic description based on Maxwell's equations, the light–matter interaction is described in the electric-dipole approximation specified by the non-linear relationship between the applied electric field **E** and induced polarization **P** as (for non-magnetic media)

$$\mathbf{P} = \epsilon_0 \left[\overleftrightarrow{\chi}^{(1)} \cdot \mathbf{E} + \overleftrightarrow{\chi}^{(2)} : \mathbf{EE} + \overleftrightarrow{\chi}^{(3)} \vdots \mathbf{EEE} + \dots \right], \quad (1)$$

written as a Taylor series in **E**. In this approach, the first term describes the linear regime at weak external fields, and $\overleftrightarrow{\chi}^{(N)}$ are the Nth-order susceptibility tensors of the rank $N + 1$, which describe the polarization-dependent parametric interaction and symmetries of the specific non-linear media. Usually, optical non-linearities of natural materials are weak, and the non-linear effects manifest themselves for strong applied electromagnetic fields, generated by powerful and coherent sources of light. Because considerable amounts of the electromagnetic energy can be confined to tiny volumes in nanoparticles or even smaller hot spots, they enable downscaling of the required optical powers, because the intensity of parametric processes scales with the fourth or sixth power of the fundamental field strength.

Under high intensities of light, an anharmonic motion of electrons produces photons at frequencies different from that of the incoming light, with SHG and third-harmonic generation (THG) as prominent examples. It is a widely adopted concept that only the electric polarization of the material is affected by the anharmonic motion of the electrons driven by the electromagnetic field. However, metamaterials can exhibit a *non-linear magnetic response*, resulting in a new type of magnetic non-linearities [69]. This picture is at large adapted in the microwave regime, and a vast number of research groups are engaged in utilizing the tailored non-linear response of metamaterials, as discussed in the recent review papers [70,71]. However, the idea of generic magnetic non-linearities remains distant to the non-linear optics community, while new direct observations of the effects induced by magnetic response are being reported, as discussed below.

An important issue in non-linear optics is crystalline symmetry. In particular, within the electric-dipole approximation of the light–matter interaction, second-order non-linear effects are not possible in uniform centrosymmetric media such as plasmonic metals and group IV semiconductors, because of the simple symmetry constraints, while no such restriction exists for third-order non-linear processes [72]. However, the inversion symmetry

can be broken at surfaces and interfaces, thus enabling the second-order non-linear processes to occur, being generated from surfaces of isotropic media due to the electric-dipole surface contribution to the effective non-linear polarization. The sensitivity of such non-linear effects to the properties of surfaces can be used in probing and sensing techniques. Importantly, the bulk non-linear polarization originates from higher-order non-local magnetic-dipole and electric-quadrupole interactions with light at the microscopic level. To account for such multipolar effects, we can present the effective light–matter interaction Hamiltonian in the form [73,74]

$$H_{\rm int} = -\mathbf{p}\cdot\mathbf{E} - \mathbf{m}\cdot\mathbf{B} - [\mathbf{Q}\nabla]\cdot\mathbf{E} - \ldots, \quad (2)$$

where **E** is a local electric field, **p** is the electric-dipole moment, **m** is the magnetic-dipole moment, and **Q** is the electric-quadrupole moment.

Strong interaction of subwavelength structures with an external light field may occur due to the resonant excitation of low-order modes (up to quadrupoles) due to *surface plasmon resonances* (in plasmonic materials, such as metals and doped graphene), or *Mie-type resonances* (in dielectric nanoparticles with high refractive index) being supported by large displacement currents. The physics of these resonances can be understood from the classical problem of Mie scattering by spherical particles. The macroscopic source of non-linear polarization is defined by the induced near-field distribution, and it is expressed in terms of multipolar bulk and surface contributions inherent to the non-linear medium. Non-linear response functions appear due to averaging multipolar light–matter interactions, which can be described by the Hamiltonian $H_{\rm int}$ at the microscopic level, accounting for the symmetry and structural properties of the material. The induced non-linear polarization generates electric and magnetic multipoles of different orders, yielding non-trivial radiation and polarization patterns through far-field interference. In the framework of this approach, the 'optical magnetic' Mie mode can support strong fields that drive the electric-dipole-allowed bulk non-linearity of the material, and in turn, the non-linear source induced in the nanoparticle can give rise to higher-order multipoles in non-linear scattering.

Non-linear effects at the nanoscale

In the last few years, the role of the non-linear magnetic response in optics has been intensively addressed. Shcherbakov *et al.* [75] employed a novel type of optically magnetic nanostructures to show that they can significantly enhance non-linear conversion; see Fig. 5(a)–(d). As mentioned above, silicon nanoparticles support the Mie-type modes including the fundamental magnetic dipolar mode. Along with being optically magnetic, they do not suffer from intrinsic losses in the infrared and are CMOS-compatible. Shcherbakov *et al.* [75] confirmed that the THG response from silicon nanodisks prevails over the THG from the bulk silicon by using THG microscopy and THG spectroscopy techniques. The low intrinsic losses of the disks made it possible to reach conversion efficiencies high enough for the generated UV light to be observed even under table-lamp illumination. Bringing the nanodisks into the oligomer arrangement provides another degree of freedom for non-linear magnetoelectric coupling [76]; see Fig. 5(e).

Similar studies of the multipolar enhancement of SHG have been conducted for hybrid metal–dielectric nanoparticles [77]. In order to straightforwardly identify the magnetic dipolar contribution to optical non-linearities, the authors performed spectrally resolved second-harmonic measurements and multipolar analysis of the SHG from a hybrid nanodisk. The latter can sustain antisymmetric movement of electron plasma leading to the resonant magnetic response. They employed the multipolar decomposition of the experimental and calculated SHG spectra, and observed that the main contribution to the detected non-linear signal originates from the conventionally neglected electric quadrupolar and magnetic dipolar sources [77].

Generation of different localized modes can reshape completely the physics of non-linear effects at the nanoscale [78]. Utilizing the Mie resonances in resonant dielectric nanoparticles has recently been recognized as a promising strategy to gain higher efficiencies of non-linear parametric processes at low modal volumes, and novel functionalities originating from optically induced magnetic response. In particular, it is possible not only to discover novel regimes of *non-linear optical magnetism* in nanoantennas [79], but also to distinguish experimentally non-linear contributions of electric and magnetic responses by analyzing the structure of polarization states of vector beams in SHG with continuous tuning of the polarization of the optical pump [79]. The electric multipoles generated can be distinguished from magnetic multipoles in the far-field region by their distinct polarization. For example, an electric-dipole polarization follows the polar angle unit vector, whereas the field generated from a magnetic-dipole mode follows the azimuthal angle unit vector. This results in 'radial' polarization from an electric dipole in the projection plane perpendicular to the dipole moment and, correspondingly,

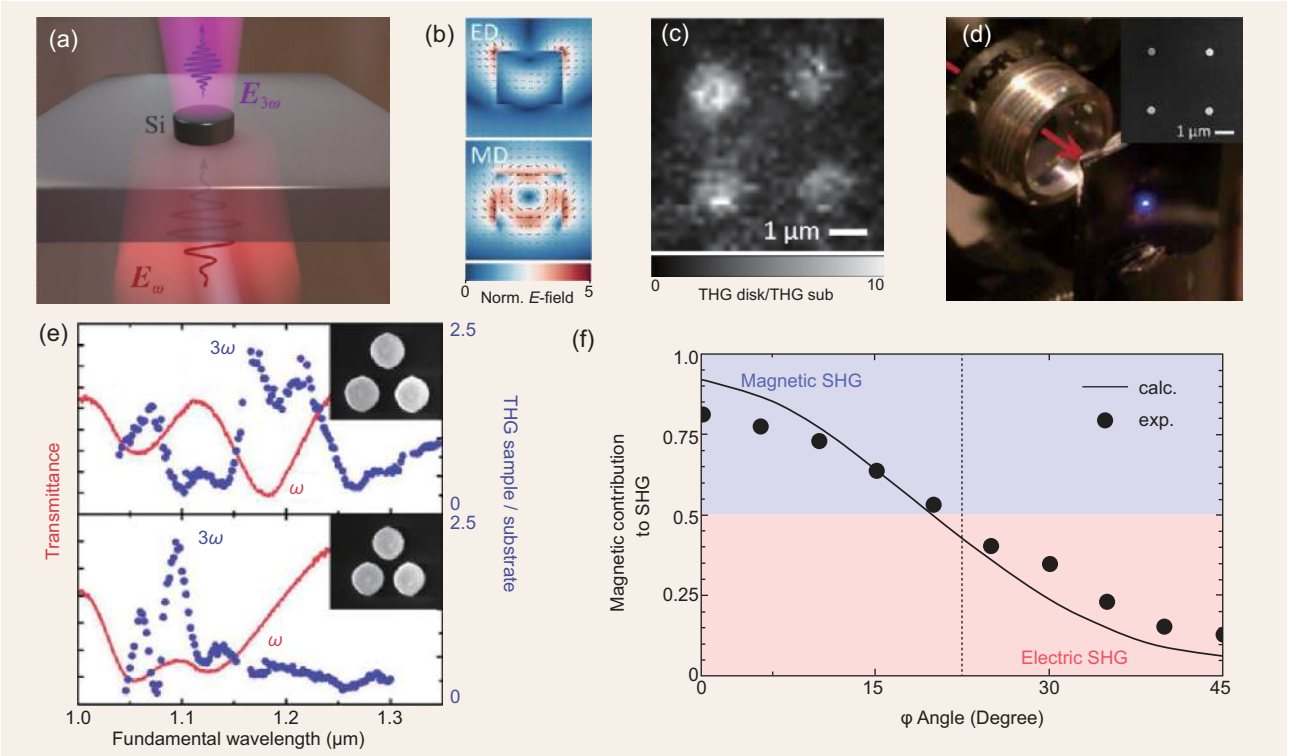

Figure 5. Non-linear harmonic generation at the nanoscale. (a)–(d) THG from an Si dielectric nanoparticle with the magnetic Mie resonance. Local fields calculated for the electric dipolar and magnetic dipolar modes, respectively. Map of the THG intensity from the nanodisks normalized over the THG from a bulk silicon slab. Eye-visible THG from the silicon nanodisk array [75]. (e) Coupling of nanodisks within oligomers tailors the non-linear optical response [76]. (f) Electric versus magnetic SHG in nanoantennas, with distinct polarization patterns for the generated electric and magnetic multipoles [79].

'azimuthal' polarization distribution from a magnetic dipole (see Fig. 5(f)).

Another important mechanism for enhancing non-linear interactions at the nanoscale is to employ multipolar interference for creating a tight field confinement in the so-called *optical anapole mode* [80,81]. This anapole mode is associated with the concept of non-radiating current configurations, and in optics it can be viewed as an engineered superposition of electric and toroidal optical dipole moments, resulting in destructive interference of the radiation fields. This may happen due to a similarity of the far-field scattering patterns generated by an optical dipole mode and toroidal modes, and, usually, for the generation of toroidal modes in metamaterials, some more complex structures of nanoparticles are suggested [82]. However, dielectric nanoparticles can support the (almost radiationless) anapole mode, allowing an overlap of the toroidal and electric-dipole modes through geometry tuning, with a pronounced dip in the far-field scattering accompanied by the specific near-field distribution [80]. Importantly, these anapole modes can be employed to resolve a major challenge with the efficient coupling of light to nanoscale optical structures. Indeed, as has been shown theoretically [81], a nanoscale laser based on a tightly confined anapole mode in InGaAs nanodisks allows the efficient coupling of light into waveguide channels with four orders of magnitude intensity compared to classical nanolasers, as well as the generation of ultrafast (of 100 fs) pulses via spontaneous mode locking of several anapoles, offering an attractive platform for integrated photonics sources for advanced and efficient nanoscale circuitry.

Recently, Grinblat *et al.* [83,84] employed the property of the anapole mode for the observation of strong third-order non-linear processes and efficient THG from Ge nanodisks. They observed a pronounced valley in the scattering cross section at the anapole mode, while the electric field energy inside the disk is maximized due to high confinement within the dielectric nanoparticle. Grinblat *et al.* [83] investigated the dependence of the third harmonic signal on the size of the nanodisk and pump wavelength and revealed the main features of the anapole mode, corresponding to an associated THG conversion efficiency of 0.0001% at an excitation wavelength of 1650 nm, which is four orders of magnitude greater than the case of an unstructured

germanium reference film. Furthermore, they concluded that the non-linear conversion via the anapole mode outperforms that via the radiative dipolar resonances by about at least one order of magnitude.

With a compact size and novel functionalities enabled by magnetic-dipole and multipolar Mie resonances, the engineered dielectric nanoparticles are perfect candidates to become important building blocks for novel and superior non-linear nanophotonic metadevices.

Non-linear metasurfaces

In the same way as conventional metamaterials can be employed to engineer non-linear optical effects [70], many metasurfaces can be used to provide an efficient control over the parameters of non-linear optical interactions to produce tunable optical devices. Moreover, as non-linear response is governed to a large extend by the effects of the field localization within nanostructures, it may provide additional information on optical properties of metasurfaces. Therefore, various parameters of the non-linear optical response such as intensity, phase and state of polarization can be effectively controlled by changing the shape anisotropy and geometry of a particular metasurface, especially important for plasmonic metamaterials [85].

Given the inherently weak non-linear response of natural materials, *non-linear metasurfaces* [86,87] can be employed to realize significant non-linear responses in much smaller volumes, with current research devoted to the quest of synthesizing novel materials with enhanced optical nonlinearities at moderate input intensities. In particular, several approaches to engineer the non-linear properties of artificial materials, metamaterials and metasurfaces have been introduced, including high-harmonic generation from ultrathin metasurfaces based on high-index dielectric resonators, as well as semiconductor-loaded metasurfaces.

One of the first demonstrations of a strong non-linear response of metasurfaces was reported [88] for n-doped multi-quantum-well semiconductor heterostructures employing intersubband transitions, with one of the largest known non-linear optical responses with a non-linear susceptibility of greater than 5×10^4 picometers per volt for second-harmonic generation under normal incidence. Such non-linear metasurfaces can be applied to engineer the Pancharatnam–Berry phase [89], thus establishing a platform to control the non-linear wavefront at will and design flat non-linear metasurfaces for efficient second-harmonic radiation, including beam steering, focusing and polarization manipulation.

The use of non-linear meta-atoms based on dielectric nanoparticles provides much higher conversion efficiencies for both second- and third-order non-linear processes. Recent studies suggest that non-linear nanoparticles can be employed for the demonstration of highly efficient all-dielectric non-linear metasurfaces. One design is *a non-linear mirror* based on the third-harmonic generation in dielectric metasurfaces that employs strong enhancement of THG in isolated silicon nanodisks optically pumped near the magnetic dipolar resonance [90]. The non-linear mirror generates a third harmonic from a laser with 1556 nm wavelength (thus, the third harmonic should be generated at 519 nm wavelength) in a way that the fundamental wave and the third harmonic are directed in opposite directions from the metasurface plane. After the interaction with the metasurface, all light at the fundamental wavelength gets reflected backward, and all light at the generated third harmonic gets transmitted forward. Such a non-linear mirror can be readily used as a frequency converter for laser cavities. The other type of non-linear mirror can act in the opposite way, transmitting light at the fundamental wavelength and directing the generated third harmonic backwards.

These very recent findings open a new direction for non-linear optics, in which phase-matching issues are relaxed, and an unprecedented level of local wavefront control is achieved over thin devices with very large non-linear responses and very low losses.

TOPOLOGICAL META-OPTICS

For decades, many branches of physics have been dominated by lattice symmetries and chemical composition as the key concepts in the classification and design of various solid-state materials. However, it has recently been demonstrated that topology may be more important than symmetry in determining certain material properties. Topology is a subtle global property of the system governing how its parts connect. Connection of two topologically distinct materials results in the formation of peculiar states at the interface between them. These topological edge states have a built-in traffic control mechanism that enforces one-way propagation of electrons along the edges or interfaces and protects electron current from scattering on impurities. Materials insulating in a bulk but conducting at the surfaces through topological edge states were discovered in solid-state physics in 2006, and they are currently known as topological insulators [91].

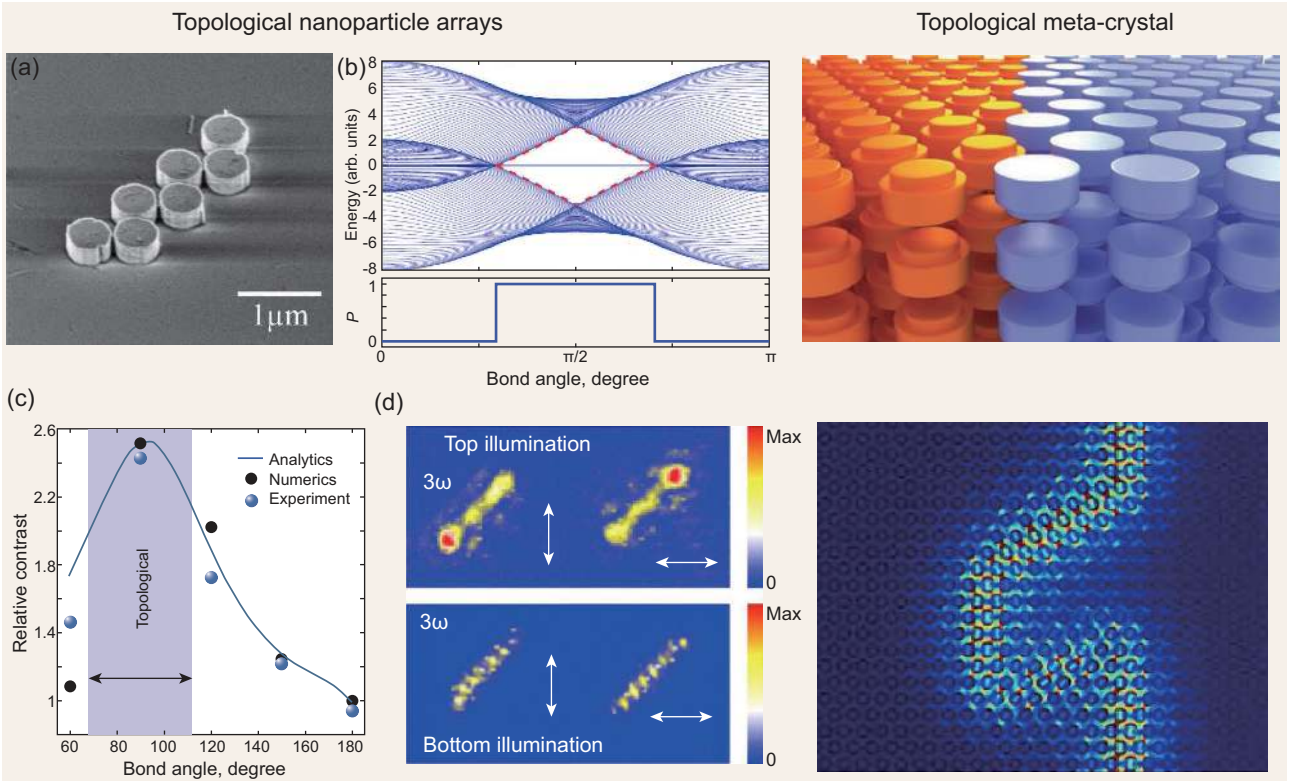

Figure 6. Topological meta-optics based on dielectric nanoparticles. Left: (a) Fabricated zigzag array of nanodisks. (b) Energy spectrum and parity of the winding number of a zigzag chain versus the angle between three consecutive particles [96]. (c) Experimental observation of the topological phase transition in zigzag arrays of nanoparticles of different lengths [99], and (d) false-color optical images of the third-harmonic radiation from a topological chain; arrows indicate polarization of pump (shown are the images for the excitation from the top and bottom, respectively) [100]. Right: 3D all-dielectric photonic topological insulator, and field distribution of the surface modes propagating without reflection across the domain wall with a sequence of sharp bends [101].

The discovery of topological insulators has triggered a vast pursuit of novel topologically protected states of light creating a new field of *topological photonics* [92,93]. In solids, such states do not conduct any bulk current but possess conducting surfaces due to topologically protected edge states [94], which can carry current without dissipation even in the presence of impurities. By now, several sophisticated designs have been developed, and unidirectional photon transport has been predicted and demonstrated [92].

Topological states of optical materials characterize the quantized global behavior of light. While first demonstrations of optical topological states were realized in systems of coupled optical waveguides [95], resonant nanophotonics allows the creation of topological states on the subwavelength scale.

Poddubny *et al.* [96] suggested the first realization of subwavelength topological states at the nanoscale. They revealed that hybridization of the polarization-degenerate modes of a zigzag chain of plasmonic nanoparticles engenders a chiral-symmetric energy spectrum. The structure exhibits a topological transition when the chain changes its structure from a line to a zigzag, as shown in Fig. 6(a). Namely, the spectrum of a straight chain is topologically trivial; it has a vanishing parity of the winding number P. For the zigzag chain this Z_2 topological invariant is non-zero (see Fig. 6(b)), being the hallmark of the edge states at both chain edges [96].

A proof-of-concept experiment confirmed the presence of edge states in the zigzag chain of gold nanodisks in the visible [97]. The chain was excited from the substrate side and near-field patterns of the plasmonic modes induced in the structure were mapped by a near-field scanning optical microscope. The measured near field demonstrates hot spots at the chain edges that were switched by rotating the polarization of the incident light.

Slobozhanyuk *et al.* [98] generalized this theory to a broader class of electromagnetic structures including dielectric nanoparticles with different symmetries of the coupled optical modes. They observed subwavelength topological edge states for electric- and magnetic-dipole and magnetic-quadrupole modes. Moreover, they demonstrated directly the robustness of the edge states against disorder [98]. These results opened novel avenues to engineering topological states of light at the nanoscale.

Later, it was established that polymeric arrays of subwavelength silicon nanodisks can support two types of topological edge modes based on *magnetic* and *electric* Mie resonances, and their topological properties are fully dictated by the spatial arrangement of the nanoparticles in the array. Kruk *et al.* [99] observed experimentally and described theoretically *topological phase transitions* at the nanoscale controlling a change from trivial to non-trivial topological states when the edge mode is excited (see Fig. 6(c)), and they traced these topological phase transitions experimentally by employing near-field scanning optical microscopy.

Recently, Kruk *et al.* [100] demonstrated topology-enhanced THG at photonic edge states in zigzag arrays of silicon nanodisks. The harmonic generation was observed only for one direction of the plane-wave excitation, manifesting the non-linearity-induced non-reciprocal nature of the photonic topological states. Figure 6(d) shows the distribution of the third-harmonic radiation across the zigzag arrays for several different polarizations of the pump. They observed experimentally localized modes at the third-harmonic frequency when the laser pump excites the topological edge states. Non-linear effects are stronger for the edge states due to a higher concentration of the electric field. The observed edge-to-center intensity contrast is about 8. Selective excitation of the left or right edges is controllable by the polarization of the pump wave (shown by arrows in Fig. 6(d)). Namely, the edge is excited when the electric field is transverse to the link between the last pair of nanodisks. The electric-dipole attribution of the edge state was confirmed by full-wave numerical simulations [100].

A zigzag array of nanoparticles provides the simplest example of a topological photonic system at the nanoscale, and it might be useful for designing fundamentally new types of photonic topological circuitry with complex magneto-electric coupling and high-intensity fields delivered on demand, not existing in any solid-state system.

More recently, a proposal was made for all-dielectric 3D *meta-crystals* consisting of resonant building blocks exhibiting electromagnetic duality between electric and magnetic fields that may be employed to create photonic topological insulators supporting propagating edge states [101]. In such systems, the magneto-electrical coupling plays the role of a synthetic gauge field that determines a topological transition to an 'insulating' regime with a complete photonic bandgap. The proposed all-dielectric meta-crystal design suggests the topological robustness of the surface states enabling reflectionless routing of electromagnetic radiation along arbitrarily shaped pathways in three dimensions (see Fig. 6, right column), which makes these modes promising for applications in photonics. This all-dielectric platform could also avoid undesirable effects such as ohmic loss, which is inevitably present in metallic and plasmonic structures.

SUMMARY AND OUTLOOK

Electromagnetic metamaterials were initially suggested for the demonstration of novel wave phenomena such as negative refraction, and later they were employed for engineering electromagnetic space with transformation optics. However, the overall demand for realistic applications of metamaterials in optics is growing, and it cannot be satisfied by conventional designs and concepts, which suffer from large losses in metallic components. The recent rapid progress in low-loss dielectric metaoptics and all-dielectric resonant nanophotonics has seen the rebirth of the metamaterial concept, and it is associated with the physics of high-index dielectric nanoparticles supporting optically induced electric and magnetic Mie resonances. This may revolutionize modern nanophotonics by bringing novel properties driven by optical magnetic response. All-dielectric resonant subwavelength structures have many advantages, including resonant behavior and low-energy dissipation into heat; they also provide the resonant enhancement of magnetic fields in dielectric components and bring new functionalities in both linear and non-linear regimes. They may also allow simpler integration approaches than plasmonic structures.

Novel opportunities are expected to appear with the use of new materials with high refractive index and low losses. In particular, the recently emerged phase-changeable materials such as GST alloys (e.g. $Ge_3Sb_2Te_6$ [102]) can be explored for mid-infrared chiral metasurfaces with tunable electric and magnetic Mie resonances, achieving multifaceted functionalities controlled by phase transitions. In addition, novel opportunities appear with the use of organic–inorganic materials [103] for developing a novel hybrid platform for non-linear optics and optoelectronics based on organic–inorganic materials combined with nanophotonic structures. Recently, it was demonstrated that metasurfaces based on nanoimprinted perovskite films optimized by alloying the organic cation part of perovskites can exhibit a significant enhancement of both linear and non-linear photoluminescence (up to 70 times) combined with advanced stability [104]. These results suggest a cost-effective approach based on nanoimprint lithography and combined with simple chemical reactions for creating a new generation of functional metasurfaces that may pave the way

toward highly efficient planar optoelectronic metadevices.

Research in the field of all-dielectric meta-optics is now moving towards tunable, non-linear and active structures and towards practical and miniature metadevices, defined as the devices having unique and useful functionalities that are realized by structuring of functional matter on the subwavelength scale. We expect that all-dielectric resonant meta-optics will ultimately employ all of the advantages of optically induced magnetic resonances and shape many important applications, including optical sensing, parametric amplification, fast spatial modulation of light for telecom applications, non-linear active media, as well as both integrated classical and quantum circuitry and topological photonics, underpinning a new generation of nanoantennas, nanolasers, highly efficient metasurfaces and ultrafast metadevices.

ACKNOWLEDGEMENTS

I thank many of my colleagues and collaborators, especially P. Belov, I. Brener, K. Chong, M. Decker, A. Fedyanin, B. Hopkins, C. Jagadish, A. Khanikaev, A. Krasnok, I. Kravchenko, S. Kruk, A. Kuznetsov, M. Limonov, W. Liu, B. Luk'yanchuk, S. Makarov, E. Melik-Gaykazyan, A. Miroshnichenko, D. Neshev, T. Pertsch, A. Poddubny, M. Rybin, M. Shcherbakov, A. Shorokhov, A. Slobozhanyuk, D. Smirnova, I. Staude and M. Tribelsky for useful discussions and fruitful collaborations. I thank A. Krasnok for his critical reading of this manuscript and useful comments. I am very much indebted to Xiang Zhang and other editors for their kind invitation.

FUNDING

This work was supported by the Australian Research Council and the ITMO University.

REFERENCES

1. Smith DR, Pendry JB and Wiltshire MCK. Metamaterials and negative refractive index. *Science* 2004; **305**: 788–92.
2. Shalaev VM. Optical negative-index metamaterials. *Nat Photon* 2007; **1**: 41–8.
3. Soukoulis CM and Wegener M. Past achievements and future challenges in the development of three-dimensional photonic metamaterials. *Nat Photon* 2011; **5**: 523–30.
4. Liu Y and Zhang X. Metamaterials: a new frontier of science and technology. *Chem Soc Rev* 2011; **40**: 2494–507.
5. Zheludev N. Obtaining optical properties on demand. *Science* 2015; **348**: 973–4.
6. Cai W, Chettar UHY and Yuan VC *et al.* Metamagnetics with rainbow colors. *Optic Express* 2007; **15**: 3333–41.
7. Alú A and Engheta N. Dynamical theory of artificial optical magnetism produced by rings of plasmonic nanoparticles. *Phys Rev B* 2008; **78**: 085112.
8. Sun L, Ma TSC and Yang DK *et al.* Interplay between optical bianisotropy and magnetism in plasmonic metamolecules. *Nano Lett* 2016; **16**: 4322–8.
9. Kante B, O'Brien K and Niv A *et al.* Proposed isotropic negative index in three-dimensional optical metamaterials. *Phys Rev B* 2012; **85**: 041103.
10. Qin L, Zhang K and Peng RW *et al.* Optical-magnetism-induced transparency in a metamaterial. *Phys Rev B* 2013; **87**: 125136.
11. Poddubny A, Iorsh I and Belov P *et al.* Hyperbolic metamaterials. *Nat Photon* 2013; **7**: 948–57.
12. Kruk SS, Wong ZJ and Pshenay-Severin E *et al.* Magnetic hyperbolic optical metamaterials. *Nat Commun* 2016; **7**: 11329.
13. Zheludev NI and Kivshar YS. From metamaterials to metadevices. *Nat Mater* 2012; **11**: 917–24.
14. Yu N and Capasso F. Flat optics with designer metasurfaces. *Nat Mater* 2014; **13**: 139–50.
15. Lalanne P and Chavel P. Metalenses at visible wavelengths: past, present, perspectives. *Laser Photon Rev* 2017. doi: 10.1002/lpor.201600295.
16. Khurgin JB. How to deal with the loss in plasmonics and metamaterials. *Nat Nanotechnol* 2015; **10**: 2–6.
17. Tassin P, Koschny T and Kafesaki M *et al.* A comparison of graphene, superconductors and metals as conductors for metamaterials and plasmonics. *Nat Photon* 2012; **6**: 259–64.
18. Boltasseva A and Atwater HA. Low-loss plasmonic metamaterials. *Science* 2011; **331**: 290–1.
19. Boltasseva A. Empowering plasmonics and metamaterials technology with new material platforms. *MRS Bull* 2014; **39**: 461–8.
20. Gregory SA, Wang Y and de Groot CH *et al.* Extreme subwavelength metal oxide direct and complementary metamaterials. *ACS Photon* 2015; **2**: 606–14.
21. Baranov DG, Zuev DA and Lepeshov SI *et al.* All-dielectric nanophotonics: the quest for better materials and fabrication techniques. *Optica* 2017; **4**: 814–25.
22. Kuznetsov AI, Miroshnichenko AE and Brongersma ML *et al.* Optically resonant dielectric nanostructures. *Science* 2016; **354**: aag2472.
23. Staude I and Schilling J. Metamaterial-inspired silicon nanophotonics. *Nat Photon* 2017; **11**: 274–84.
24. Yang ZJ, Jiang R and Zhuo X *et al.* Dielectric nanoresonators for light manipulation. *Phys Rep* 2017; **701**: 1–50.
25. Kruk S and Kivshar YS. Functional meta-optics and nanophotonics governed by Mie resonances. *ACS Photon* 2017; **4**: 2638–49.
26. Mie G. Beiträge zur Optik trüber Medien, speziell kolloidaler Metallösungen. *Ann Phys* 1908; **330**: 377.
27. Hopkins B, Miroshnichenko A and Kivshar Y. All-dielectric nanophotonic structures: exploring the magnetic component of light. In: Agrawal A, Benson T and de la Rue R *et al.* (eds). *Recent Trends in Computational Photonics*. Berlin: Springer, 2017.
28. Evlyukhin AB, Reinhardt C and Seidel A *et al.* Optical response features of Si-nanoparticle arrays. *Phys Rev B* 2010; **82**: 045404.
29. Kivshar Y and Miroshnichenko A. Meta-optics with Mie resonances. *Optic Photon News* 2017; **28**: 24–31.

30. Kuznetsov AI, Miroshnichenko AE and Fu YH *et al.* Magnetic light. *Sci Rep* 2012; **2**: 492.
31. Evlyukhin AB, Novikov SM and Zywietz U *et al.* Demonstration of magnetic dipole resonances of dielectric nanospheres in the visible region. *Nano Lett* 2012; **12**: 3749–55.
32. Liu W and Kivshar YS. Multipolar interference effects in nanophotonics. *Phil Trans R Soc A* 2017; **375**: 20160317.
33. Miroshnichenko AE, Lukyanchuk B and Maier SA *et al.* Optically induced interaction of magnetic moments in hybrid metamaterials. *ACS Nano* 2012; **6**: 837–42.
34. Miroshnichenko AE, Filonov DB and Luk'yanchuk Y *et al.* Antiferromagnetic order in hybrid electromagnetic metamaterials. *New J Phys* 2017; **19**: 083013.
35. Luk'yanchuk B, Zheludev NI and Maier SA *et al.* The Fano resonance in plasmonic nanostructures and metamaterials. *Nat Mater* 2010; **9**: 707–15.
36. Miroshnichenko AE and Kivshar YS. Fano resonances in all-dielectric oligomers. *Nano Lett* 2012; **12**: 6459–63.
37. Hopkins B, Poddubny AN and Miroshnichenko AE. Revisiting the physics of Fano resonances for nanoparticle oligomers. *Phys Rev A* 2013; **88**: 053819.
38. Limonov MF, Rybin MV and Poddubny AN *et al.* Fano resonances in photonics. *Nat Photon* 2017; **11**: 543–54.
39. Kerker M. *The Scattering of Light and Other Electromagnetic Radiation*. New York: Academic Press, 1969.
40. Liu W, Miroshnichenko AE and Neshev D *et al.* Broadband unidirectional scattering by magneto-electric core–shell nanoparticles. *ACS Nano* 2012; **6**: 5489–97.
41. Krasnok AE, Miroshnichenko AE and Belov PA *et al.* Huygens optical elements and Yagi'Uda nanoantennas based on dielectric nanoparticles. *JETP Lett* 2011; **94**: 593–8.
42. Krasnok AE, Miroshnichenko AE and Belov P *et al.* All-dielectric optical nanoantennas. *Optic Express* 2012; **20**: 20599–604.
43. Fu YH, Kuznetsov AI and Miroshnichenko AE *et al.* Directional visible light scattering by silicon nanoparticles. *Nat Commun* 2013; **4**: 1527.
44. Person S, Jain M and Lapin Z *et al.* Demonstration of zero optical backscattering from single nanoparticles. *Nano Lett* 2013; **13**: 1806–9.
45. Staude I, Miroshnichenko AE and Decker M *et al.* Tailoring directional scattering through magnetic and electric resonances in subwavelength silicon nanodisks. *ACS Nano* 2013; **7**: 7824–32.
46. Gefferin JM, García-Cámara B and Gomez-Medina R *et al.* Magnetic and electric coherence in forward- and back-scattered electromagnetic waves by a single dielectric subwavelength sphere. *Nat Commun* 2012; **3**: 1171.
47. Decker M, Staude I and Falkner M *et al.* High-efficiency dielectric Huygens' surfaces. *Adv Opt Mater* 2015; **3**: 813–20.
48. Chong KE, Staude I and James A *et al.* Polarization-independent silicon metadevices for efficient optical wavefront control. *Nano Lett* 2015; **15**: 5369–74.
49. Chong KE, Wang L and Staude I *et al.* Efficient polarization-insensitive complex wavefront control using Huygens' metasurfaces based on dielectric resonant meta-atoms. *ACS Photon* 2016; **3**: 514–9.
50. Vo S, Fattel D and Sorin WV *et al.* Sub-wavelength grating lenses with a twist. *IEEE Photon Tech Lett* 2014; **26**: 1375–8.
51. Chen BH, Wu PC and Su V *et al.* GaN metalens for pixel-level full-color routing at visible light. *Nano Lett* 2017; **17**: 6345–52.
52. Sautter J, Staude I and Decker M *et al.* Active tuning of all-dielectric metasurfaces. *ACS Nano* 2015; **9**: 4308–15.
53. Moitra P, Slovick BA and Li II *et al.* Large-scale all-dielectric metamaterial perfect reflectors. *ACS Photon* 2015; **2**: 692–8.
54. Carpenter J, Eggleton BJ and Schröder J. Observation of Eisenbud-Wigner-Smith states as principal modes in multimode fibre. *Nat Photon* 2015; **9**: 751.
55. Xie G, Li L and Ren Y *et al.* Performance metrics and design considerations for a free-space optical orbital-angular-momentum-multiplexed communication link. *Optica* 2015; **2**: 357–65.
56. Kruk S, Ferreira F and Mac-Suibhne N *et al.* Highly transparent dielectric metasurfaces for fast mode modulation and spatial multiplexing. *Laser Photon Rev* 2018; in press.
57. Wang L, Kruk S and Tang H *et al.* Grayscale transparent metasurface holograms. *Optica* 2016; **3**: 1504–5.
58. Proust J, Bedu F and Gallas B *et al.* All-dielectric colored metasurfaces with silicon Mie resonances. *ACS Nano* 2016; **10**: 7761–7.
59. Flauraud V, Reyes M and Paniague-Domínquez R *et al.* Silicon nanostructures for bright field full color print. *ACS Photon* 2017; **4**: 1913–9.
60. Sun S, Zhou Z and Zhang C *et al.* All-dielectric full-color printing with TiO_2 metasurfaces. *ACS Nano* 2017; **11**: 4445–52.
61. Zhu X, Yan W and Levy U *et al.* Resonant laser printing of structural colors on high-index dielectric metasurfaces. *Sci Adv* 2017; **3**: e1602487.
62. O'Brian S and Pendry JB. Photonic band-gap effects and magnetic activity in dielectric composites. *J Phys Condens Matter* 2002; **14**: 4035–44.
63. Vynck K, Felbacq D and Centeno E *et al.* All-dielectric rod-type metamaterials at optical frequencies. *Phys Rev Lett* 2009; **102**: 133901.
64. Peng L, Ran L and Chen H *et al.* Experimental observation of left-handed behavior in an array of standard dielectric resonators. *Phys Rev Lett* 2007; **98**: 157403.
65. Zhao Q, Kang L and Du B *et al.* Experimental demonstration of isotropic negative permeability in a three-dimensional dielectric composite. *Phys Rev Lett* 2008; **101**: 027402.
66. Zhao Q, Zhou J and Lippens D. Mie resonance-based dielectric metamaterials. *Mater Today* 2009; **12**: 60.
67. Rybin MV, Filonov DS and Samusev KB *et al.* Phase diagram for the transition from photonic crystals to dielectric metamaterials. *Nat Commun* 2015; **6**: 10102.
68. Neshev D, Camacho-Morales R and Rahmani M *et al.* Manipulating second-harmonic light from semiconductor nanocrystals. *SPIE Newsroom* 2017. doi: 10.1117/2.1201705.006852.
69. Rose A, Huang D and Smith DR. Nonlinear interference and unidirectional wave mixing in metamaterials. *Phys Rev Lett* 2013; **110**: 063901.
70. Lapine M, Shadrivov I and Kivshar Y. Nonlinear metamaterials. *Rev Mod Phys* 2014; **86**: 1093–123 and references therein.
71. Lapine M. New degrees of freedom in nonlinear metamaterials. *Phys Status Solidi B* 2017; **254**: 1600452 and references therein.
72. Lippitz M, van Dijk MA and Orrit M. Third-harmonic generation from single gold nanoparticles. *Nano Lett* 2005; **5**: 799–802.
73. Novotny L and Hecht B. *Principles of Nano-Optics*. New York: Cambridge University Press, 2007.
74. Kasperczyk M, Person S and Ananias D *et al.* Excitation of magnetic dipole transitions at optical frequencies. *Phys Rev Lett* 2015; **114**: 163903.
75. Shcherbakov MR, Neshev DN and Hopkins B *et al.* Enhanced third-harmonic generation in silicon nanoparticles driven by magnetic response. *Nano Lett* 2014; **14**: 6488–92.
76. Shcherbakov MR, Shorokhov AS and Neshev DN *et al.* Nonlinear interference and tailorable third-harmonic generation from dielectric oligomers. *ACS Photon* 2015; **2**: 578–82.

77. Kruk SS, Weismann M and Bykov AY *et al.* Enhanced magnetic second-harmonic generation from resonant metasurfaces. *ACS Photon* 2015; **2**: 1007–12.
78. Smirnova D and Kivshar YS. Multipolar nonlinear nanophotonics. *Optica* 2016; **3**: 1241–55.
79. Kruk S, Camacho-Morales R and Xu L *et al.* Nonlinear optical magnetism revealed by second-harmonic generation in nanoantennas. *Nano Lett* 2017; **17**: 3914–8.
80. Miroshnichenko AE, Evlyukhin AB and Yu YF *et al.* Anapole modes in dielectric nanoparticles. *Nat Commun* 2015; **6**: 8069.
81. Totero Gongora JS, Miroshnichenko AE and Kivshar YS *et al.* Anapole nanolasers for mode-locking and ultrafast pulse generation. *Nat Commun* 2017; **8**: 15535.
82. Kaelberer T, Fedotov VA and Papasimakis N *et al.* Toroidal dipolar response in a metamaterial. *Science* 2010; **330**: 1510–2.
83. Grinblat G, Li Y and Nielsen MP *et al.* Enhanced third-harmonic generation in single Germanium nanodisks excited at the anapole mode. *Nano Lett* 2016; **16**: 4635–40.
84. Grinblat G, Li Y and Nielsen MP *et al.* Efficient third harmonic generation and nonlinear subwavelength imaging at a higher-order anapole mode in a single germanium nanodisk. *ACS Nano* 2017; **11**: 953–60.
85. Minovich AE, Miroshnichenko AE and Bykov AY *et al.* Functional and nonlinear optical metasurfaces. *Laser Photon Rev* 2015; **9**: 195–213.
86. Li G, Zhang S and Zentgraf T. Nonlinear photonic metasurfaces. *Nat Rev Mater* 2017; **2**: 17010.
87. Krasnok A, Tymchenko M and Alú A. Nonlinear metasurfaces: a paradigm shift in nonlinear optics. *Mater Today* 2017. doi: 10.1016/j.mattod.2017.06.007.
88. Lee J, Tymchenko M and Argyropoulos C *et al.* Giant nonlinear response from plasmonic metasurfaces coupled to intersubband transitions. *Nature* 2014; **511**: 65–9.
89. Tymchenko M, Gomez-Diaz JS and Lee J *et al.* Gradient nonlinear Pancharatnam-Berry metasurfaces. *Phys Rev Lett* 2015; **115**: 207403.
90. Wang L, Xu L and Kruk SS *et al.* Nonlinear mirror with all-dielectric metasurface. *The European Conference on Lasers and Electro-Optics 2017*, Munich, 25–29 June 2017.
91. Bernevig B and Hughes T. *Topological Insulators and Topological Superconductors*. Princeton: Princeton University Press, 2013.
92. Lu L, Joannopoulos JD and Soljačić M. Topological photonics. *Nat Photon* 2014; **8**: 821–9.
93. Sun XC, He C and Liu XP *et al.* Two-dimensional topological photonic systems. *Prog Quantum Electron* 2017; **55**: 52–73.
94. Hasan MZ and Kane CL. Topological insulators. *Rev Mod Phys* 2010; **82**: 3045–67.
95. Hafezi M, Mittal S and Fan J *et al.* Imaging topological edge states in silicon photonics. *Nat Photon* 2013; **7**: 1001–5.
96. Poddubny A, Miroshnichenko A and Slobozhanyuk A *et al.* Topological Majorana states in zigzag chains of plasmonic nanoparticles. *ACS Photon* 2014; **1**: 101–5.
97. Sinev IS, Mukhin IS and Slobozhanyuk AP *et al.* Mapping plasmonic topological states at the nanoscale. *Nanoscale* 2015; **7**: 11904–8.
98. Slobozhanyuk AP, Poddubny AN and Miroshnichenko AE *et al.* Subwavelength topological edge states in optically resonant dielectric structures. *Phys Rev Lett* 2015; **114**: 123901.
99. Kruk S, Slobozhanyuk A and Denkova D *et al.* Edge states and topological phase transitions in chains of dielectric nanoparticles. *Small* 2017. doi: 10.1002/smll.201603190.
100. Kruk SS, Slobozhanyuk A and Shorokhov A *et al.* Third-harmonic generation from photonic topological states in zigzag nanodisks. In: *OSA Frontiers in Optics/Laser Science Conference (FiO/LS). Postdeadline paper FTh4B.2.* Washington, DC, 18–21 September 2017.
101. Slobozhanyuk A, Mousavi SH and Ni X *et al.* Three-dimensional all-dielectric photonic topological insulator. *Nat Photon* 2016; **11**: 130–6.
102. Chu CH, Tseng ML and Chen J *et al.* Active dielectric metasurface based on phase-change medium. *Laser Photon Rev* 2016; **10**: 986–94.
103. Sutherland BR and Sargent EH. Perovskite photonic sources. *Nat Photon* 2016; **10**: 295–302.
104. Makarov SV, Milichko V and Ushakova EV *et al.* Multifold emission enhancement in nanoimprinted hybrid perovskite metasurfaces. *ACS Photon* 2017; **4**: 728–35.